

# Connectivity between Eurasian snow cover extent and Canadian snow water equivalent and river discharge

Stephen J. Déry<sup>1</sup>

Program in Atmospheric and Oceanic Sciences, Princeton University, Princeton, New Jersey, USA

Justin Sheffield and Eric F. Wood

Department of Civil and Environmental Engineering, Princeton University, Princeton, New Jersey, USA

Received 3 May 2005; revised 28 July 2005; accepted 30 August 2005; published 6 December 2005.

[1] We explore pan-Arctic climate connectivity by examining historical time series of satellite-based measurements of Eurasian snow cover extent and of observed Canadian snow water equivalent (SWE) and freshwater discharge, with a focus on the Churchill River Basin of Labrador and the Chesterfield Inlet Basin of Nunavut. Analysis of the data reveals statistically significant positive (negative) correlations between spring and summer Eurasian standardized snow cover extent anomalies and annual maximum monthly SWE as well as freshwater discharge in the Churchill River (Chesterfield Inlet) Basin the following year. A spatially coherent response to the forcing is observed since 19 rivers draining more than  $0.6 \times 10^6 \text{ km}^2$  of northern Quebec and Labrador and with a mean annual total discharge of  $320 \text{ km}^3 \text{ yr}^{-1}$  show statistically significant positive correlations to the annual Eurasian standardized snow cover extent anomalies. The origin of this pan-Arctic climate connectivity is related to the persistent nature of the Eurasian snow cover extent anomalies and the associated accumulated gains or deficits in the surface radiation and water budgets that impose a memory in the climate system. The Eurasian snow cover extent anomalies provide some degree of predictability (up to 1 year in advance) of the surface water budget in the Churchill River and Chesterfield Inlet Basins. They further suggest that a declining trend in Eurasian snow cover extent will yield decreasing (increasing) SWE and river discharge in the Churchill River (Chesterfield Inlet) Basin in the 21st century.

**Citation:** Déry, S. J., J. Sheffield, and E. F. Wood (2005), Connectivity between Eurasian snow cover extent and Canadian snow water equivalent and river discharge, *J. Geophys. Res.*, 110, D23106, doi:10.1029/2005JD006173.

## 1. Introduction

[2] Of all regions on Earth, the pan-Arctic domain is expected to experience some of the more pronounced climatic and environmental changes in the 21st century [Holland and Bitz, 2003]. The retreat and thinning of the snow and ice covers induces a positive feedback (the so-called “snow/ice–albedo feedback”) that accentuates warming at high latitudes [Cess *et al.*, 1991]. As a result, warming in the northern polar regions will increase at a rate of 1.5 to 4.5 greater than the remainder of the Northern Hemisphere [Holland and Bitz, 2003].

[3] Although our knowledge of polar processes has improved in recent years, the existence and degree of pan-Arctic climate connectivity is not well known. Teleconnection patterns imply that the state of the atmosphere, ocean,

and land surface at remote locations (from the midlatitudes to the tropics) can impact conditions at high northern latitudes; conversely, the state of the pan-Arctic domain can influence regions further to the south. If the pan-Arctic undergoes some of the most pronounced changes on the planet as a result of global warming, then its effects may be felt worldwide.

[4] Snow constitutes one of the most prominent and transient features of the pan-Arctic domain. Snow covers on average  $46 \times 10^6 \text{ km}^2$  of the Northern Hemisphere land surface during January and  $4 \times 10^6 \text{ km}^2$  during August [Frei and Robinson, 1999]. The high albedo and emissivity of snow, its low thermal conductivity, and its ability to act as a heat sink through sublimation and melting processes imply that snow cover forms a distinctive land surface feature [Cohen and Rind, 1991; Déry and Yau, 2002; Déry *et al.*, 2005a]. When anomalies in snow cover arise, the atmosphere and land surface also change. The presence of a snow cover cools the overlying atmosphere and warms the underlying ground [Ellis and Leathers, 1998; Stieglitz *et al.*, 2001, 2003]. An increase in snow mass also leads to excess

<sup>1</sup>Now at Environmental Science and Engineering Program, University of Northern British Columbia, Prince George, British Columbia, Canada.

soil moisture after the spring melt [Yeh *et al.*, 1983; Barnett *et al.*, 1989; Shinoda, 2001]. Furthermore, positive snow water equivalent (SWE) anomalies enhance freshwater discharge, especially in high-latitude and/or high-altitude river basins, where meltwater contributes as much as 80% of the annual streamflow [McNamara *et al.*, 1998; Déry *et al.*, 2005b].

[5] Fluctuations in snow cover extent vary considerably in both space and time, especially during the transition seasons of spring and fall [Robinson and Frei, 2000; Dye, 2002; Déry *et al.*, 2004]. Continental-scale snow anomalies substantially affect the surface radiation and water budgets, particularly during spring and early summer [Yeh *et al.*, 1983; Barnett *et al.*, 1989; Groisman *et al.*, 1994a, 1994b; Pielke *et al.*, 2000]. In turn, this may impact remote locations through large-scale teleconnections. A well-known relation exists between Eurasian snow cover extent anomalies and the Indian summer monsoon [Hahn and Shukla, 1976; Barnett *et al.*, 1988, 1989; Bamzai and Shukla, 1999]. Barnett *et al.* [1988, 1989] further noted an intercontinental teleconnection between simulated spring SWE and soil moisture anomalies in Eurasia and meteorological fields in North America. More recent work has focused on the link between boreal summer/fall snow cover extent anomalies in Eurasia and the Arctic Oscillation (AO) or the North Atlantic Oscillation (NAO). The AO is the dominant mode of interannual variability in the Northern Hemisphere as represented by the leading empirical orthogonal function of mean sea level pressure (SLP) above 20°N [Thompson and Wallace, 1998]. The NAO is defined as the standardized difference in SLP between locations in Iceland and southwestern Europe (usually the Azores or Lisbon, Portugal) and is often considered as a regional manifestation of the AO [Hurrell, 1995].

[6] Observational analyses and modeling studies reveal a link between Northern Hemisphere snow cover extent anomalies and the AO/NAO. Watanabe and Nitta [1998, 1999] determine that large Eurasian snow cover extent anomalies during the fall of 1976 and 1988 amplified shifts in the large-scale atmospheric circulation including the NAO. Using an ensemble of ECHAM3 global climate simulations, Gong *et al.* [2003a, 2003b] demonstrate that the modeled atmospheric state responds to a positive snow cover extent anomaly during fall (SON) in Eurasia by weakening the AO during the subsequent winter (DJF) months. Furthermore, Saunders *et al.* [2003] find that summer snow cover extent anomalies in North America and Eurasia are significantly linked to the upcoming winter NAO. Bojariu and Gimeno [2003] argue that the interaction between Eurasian snow cover extent and the NAO leads to a mechanism promoting their multiannual persistence of a given polarity. Qian and Saunders [2003] exploit the link between summer snow cover extent anomalies and the NAO to successfully hindcast wintertime storminess over the North Atlantic. Cohen and Saito [2003] employ a similar methodology to determine that summer and fall snow cover extent anomalies in Eurasia have better predictive skill of eastern United States winter surface air temperatures (SATs) than the AO/NAO.

[7] Although summer and fall snow cover extent anomalies constitute a possible mechanism in forcing the AO/NAO, other work shows that the winter AO leads Northern

Hemisphere snow cover extent anomalies [Bamzai, 2003; Saito and Cohen, 2003]. Bamzai [2003] and Schaefer *et al.* [2004] find that the winter AO influences the timing of spring melt dates in Europe. Since meltwater drives the annual freshet in most pan-Arctic watersheds, links between the AO/NAO and river discharge may also exist. For instance, a twentieth century positive trend in the NAO coincides with increasing river discharge to the Arctic Ocean [Peterson *et al.*, 2002]. Déry and Wood [2004] find that the AO explains with statistical significance up to 90% of the recent variability of river discharge into Hudson Bay.

[8] These studies provide evidence that Eurasian snow anomalies play a key role in pan-Arctic climate connectivity. However, the degree to which the Eurasian snow anomalies affect the terrestrial water budget in Canada remains unknown. The goal of this study, therefore, is to explore the relationship between measured Eurasian snow cover extent anomalies and observed Canadian SWE and river discharge anomalies and to discuss the physical mechanism behind this teleconnectivity (if and where it exists). The remainder of the paper first introduces the data sets and methods used in the study. Results are then presented prior to a discussion on the physical mechanism responsible for pan-Arctic climate connectivity and on the potential predictability of Canadian SWE and river discharge anomalies. The paper ends with a summary of our findings.

## 2. Data Sets and Methods

### 2.1. Data Sets

[9] Several observational data sets are used in this work to investigate pan-Arctic climate connectivity from different perspectives. Coherent signals inferred from independent, observational data sets enhance confidence on the existence of the associated links. The following is a summary of the four quality-controlled data sets employed in the present study:

[10] 1. Monthly mean snow cover extent data for Eurasia covering the period 1973–2003 from the National Oceanic and Atmospheric Administration's (NOAA's) Climate Prediction Center are employed (available online at <http://www.cpc.ncep.noaa.gov/data/snow/>). The snow cover extent data are inferred from satellite measurements and are considered reliable over the period of record although uncertainties in the data exist, especially during spring over northern Canada and perhaps Eurasia as well [Wang *et al.*, 2005]. In addition, anomalies are most sensitive to errors during summer when the Eurasian snow cover extent attains its annual minimum. Care must therefore be taken in analyzing and interpreting results using only spring and summer Eurasian snow cover extent measurements. To minimize the influence of these uncertainties on our results, North American snow cover extent data are excluded from the analyses and both monthly and annual anomalies in Eurasian snow cover extent data are used to infer its connectivity with Canadian SWE and river discharge.

[11] 2. Monthly mean SWE (in millimeters) data at a resolution of 0.3° from the Canadian Meteorological Centre for the period 1980–1997 [Brown *et al.*, 2003]. The SWE data encompass all of North America and are based on ≈8000 daily observations and a snow accumulation, aging,

and ablation model driven by the European Centre for Medium-Range Weather Forecasts (ECMWF) Reanalysis (ERA-15) data set. Owing to the sparsity of observing stations above 55°N, the SWE data for northern Canada are based largely on the snow model developed by *Brown et al.* [2003]. Here, we use the annual maximum monthly SWE since this quantity represents the time-integrated wintertime precipitation.

[12] 3. Canadian records of daily river discharge are extracted from the Water Survey of Canada's Hydrometric Database (HYDAT; available online at <http://www.wsc.ec.gc.ca/>). From HYDAT, *Déry et al.* [2005c] and *Déry and Wood* [2005] constructed time series of daily, monthly, and annual freshwater discharge rates for 64 rivers of northern Canada covering the period 1964–2003. This work focuses on two of these watersheds, namely the Churchill River Basin of Labrador and the Chesterfield Inlet Basin (including the contributions from the Thelon, Dubawnt, Kazan, and Quoich Rivers) in Nunavut. These two river basins are selected owing to the availability of good, long-term records of discharge data, their relatively large contributing areas and annual volumetric flows, and the substantial role of snow in the hydrology of these watersheds. As shown later, the Churchill River and Chesterfield Inlet Basins also exhibit strong hydrological responses to the Eurasian snow cover extent anomalies. Results are then generalized to the other 62 rivers of northern Canada investigated by *Déry and Wood* [2005].

[13] 4. Six-hourly global meteorological data at a horizontal resolution of 2.5° are provided by the ERA-40 data set (available online at [http://data.ecmwf.int/data/d/era40\\_daily/](http://data.ecmwf.int/data/d/era40_daily/)). These meteorological data were generated using a “frozen version” of a numerical weather prediction model in a constant analysis framework. Fields used in the present work include SLP, 500 hPa geopotential height (H5), SAT, and snowfall. *Déry and Wood* [2004] concluded that the ERA-40 data compared well with observations of SAT and precipitation in the Hudson Bay Basin and hence can be used with confidence over northern Canada.

## 2.2. Methods

[14] Although teleconnections span wide regions of the globe, this study centers on the role of Eurasian snow cover extent anomalies on Canadian SWE and river discharge anomalies. The period of interest spans 1973–2003, although some analyses are restricted to 1980–1997 owing to the shorter time series of the SWE data.

[15] Prior to the statistical analyses, the time series of monthly mean snow cover extent  $S_E$ , annual maximum monthly SWE or snow mass  $S_M$ , and monthly or annual river discharge rate  $D$  are all standardized (SVA<sub>*i*</sub>) such that

$$\text{SVA}_i = \frac{V_i - \overline{V}_i}{\sigma_V} \quad (1)$$

where the overbar denotes the mean monthly or annual value of the given variable  $V$  ( $S_E$ ,  $S_M$ , or  $D$ ),  $\sigma_V$  represents its monthly or annual standard deviation over the period of record, and where the subscript  $i$  denotes a given month or year.

[16] Common statistical tests, including Pearson's correlation coefficient between two variables, are then per-

formed. The Eurasian standardized snow cover extent are correlated to the Canadian standardized SWE and river discharge anomalies, with a focus on the Churchill River and Chesterfield Inlet Basins. Time lags or leads (from 0 to 12 months) are imposed in the calculations to determine possible causal relationships. Only correlation coefficients with  $p < 0.05$  are considered statistically significant in this study.

## 3. Results

[17] In this study, we explore how Eurasian snow cover extent anomalies affect Canadian SWE and river discharge anomalies. We first present individually the historical time series of Eurasian standardized snow cover extent anomalies and Canadian standardized SWE and river discharge anomalies. Two watersheds of northern Canada, the Churchill River and the Chesterfield Inlet Basins, are selected for more detailed analyses. The historical time series are then used to determine the connectivity between Eurasian snow cover extent anomalies and Canadian SWE and river discharge anomalies. Two years with pronounced Eurasian snow cover extent anomalies are then investigated to establish the response of the pan-Arctic climate system to large and persistent positive (1979/80) and negative (1988/89) Eurasian snow cover extent anomalies.

### 3.1. Historical Trends in Eurasian Snow Cover Extent Anomalies and in Canadian SWE and River Discharge Anomalies

[18] Figure 1 illustrates the time series of monthly standardized snow cover extent anomalies in Eurasia from 1973 to 2003. Large, positive snow cover extent anomalies occurred in the late 1970s and early 1980s, with the exception of large, negative anomalies for the winters of 1980 and 1981. After a period of low variability, prominent negative snow cover extent anomalies arose from 1988 to 1995, and again from 1999 to 2002.

[19] The mean annual maximum monthly SWE for Canada over the period 1980–1997 based on the *Brown et al.* [2003] data set is shown in Figure 2. Maximum values are found in western and eastern Canada, with lower values in central and northern Canada. This is in accord with the climatological snow water equivalent for March derived from passive microwave data [*Derksen et al.*, 2005]. Snowfall is considerably higher in Labrador than in Nunavut owing to its proximity to a major wintertime storm track [*Zishka and Smith*, 1980] and to the North Atlantic Ocean, among other factors.

[20] The mean annual freshwater discharge rates for the Churchill River and Chesterfield Inlet Basins are 57.9 and 48.6 km<sup>3</sup> yr<sup>-1</sup>, respectively (see Table 1). These rivers therefore rank among the top 10 largest by annual mean flow in northern Canada [*Déry et al.*, 2005c; *Déry and Wood*, 2005]. Discharge rates per contributing area and the mean annual maximum monthly SWE for the Churchill River Basin surpass by a factor of 3 those for the Chesterfield Inlet. The ratio of mean annual maximum monthly SWE to river discharge approaches 40% in the two watersheds.

[21] Figure 3 depicts the monthly standardized discharge anomalies for the Churchill River and Chesterfield Inlet Basins over the period 1973–2003. Also plotted in

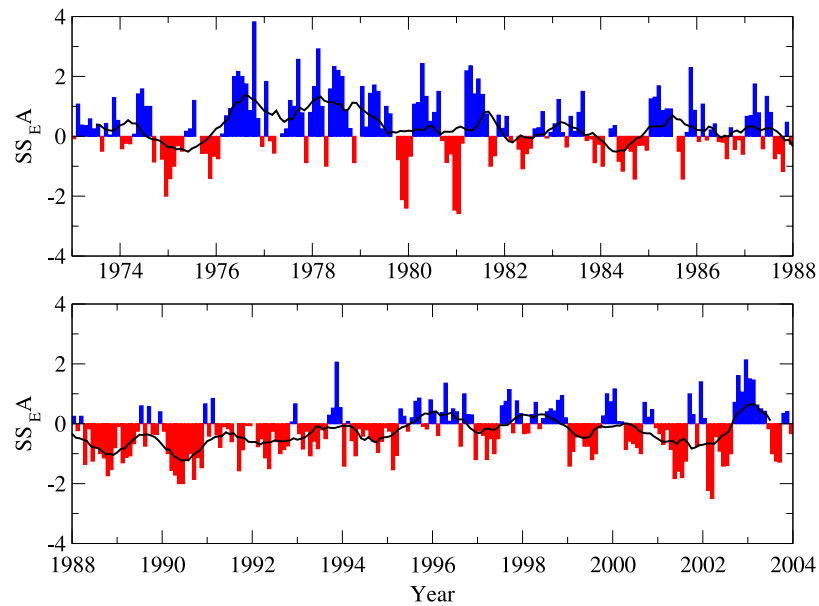


**Figure 1.** Monthly standardized snow cover extent ( $SS_{EA}$ ) anomalies in Eurasia, 1973–2003. Blue (red) bars denote positive (negative) anomalies, and the black lines depict a 12-month running mean.

Figure 3 are the annual standardized maximum monthly SWE anomalies between 1980 and 1997. The seasonal maximum SWE integrates wintertime precipitation and provides an indication of the subsequent river discharge

anomalies. For instance, large positive (negative) SWE anomalies in the Churchill River Basin (Chesterfield Inlet Basin) in the early 1980s are associated with positive (negative) streamflow anomalies.

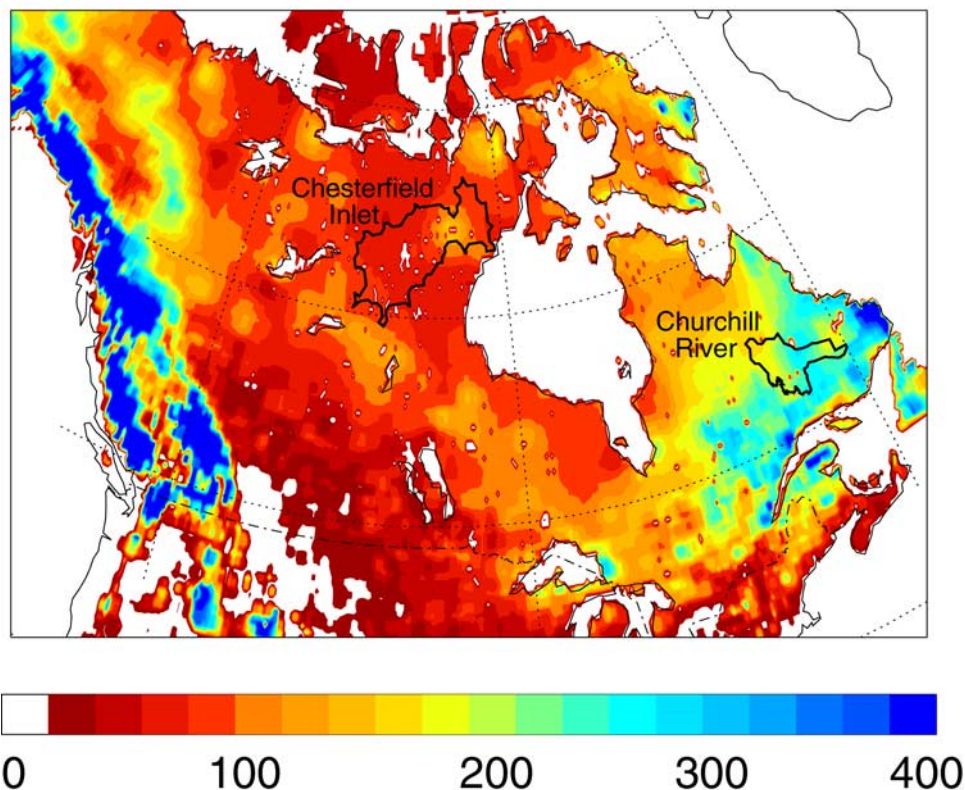


**Figure 2.** Mean annual maximum monthly SWE (millimeters) in Canada, 1980–1997. Thick black lines delineate the Churchill River Basin of Labrador and the Chesterfield Inlet Basin of Nunavut. The outline of the Churchill River Basin only depicts the gauged area and therefore shows no outlet to the Atlantic Ocean.

**Table 1.** Details of the Two River Basins of Northern Canada Investigated in This Study<sup>a</sup>

Basin	Latitude, °N	Longitude, °W	Area, km <sup>2</sup>	$D$ , km <sup>3</sup>	$D$ , mm	$S_M$ , mm SWE	$S_M/D$ , %
Chesterfield Inlet	63.70	90.62	259,979.	48.6	187.1	83.7	44.7
Churchill River	53.24	60.79	92,500.	57.9	626.4	239.8	38.3

<sup>a</sup>Information listed includes the geographical coordinates of the recording gauge nearest to the river's outlet, the contributing area that is gauged, the mean annual river discharge rate  $D$  (1973–2003), and the mean annual maximum monthly SWE  $S_M$  (1980–1997).

### 3.2. Connectivity Between Eurasian Snow Cover Extent Anomalies and Canadian SWE and River Discharge Anomalies

[22] Figure 4 shows the correlation coefficient between Eurasian snow cover extent anomalies in April, June,

August, and October and the annual maximum SWE anomaly over Canada the following winter for the period 1980–1997. These months are chosen since spring to autumn Eurasian snow cover extent anomalies correlate significantly with the AO/NAO [Bojariu and Gimeno,

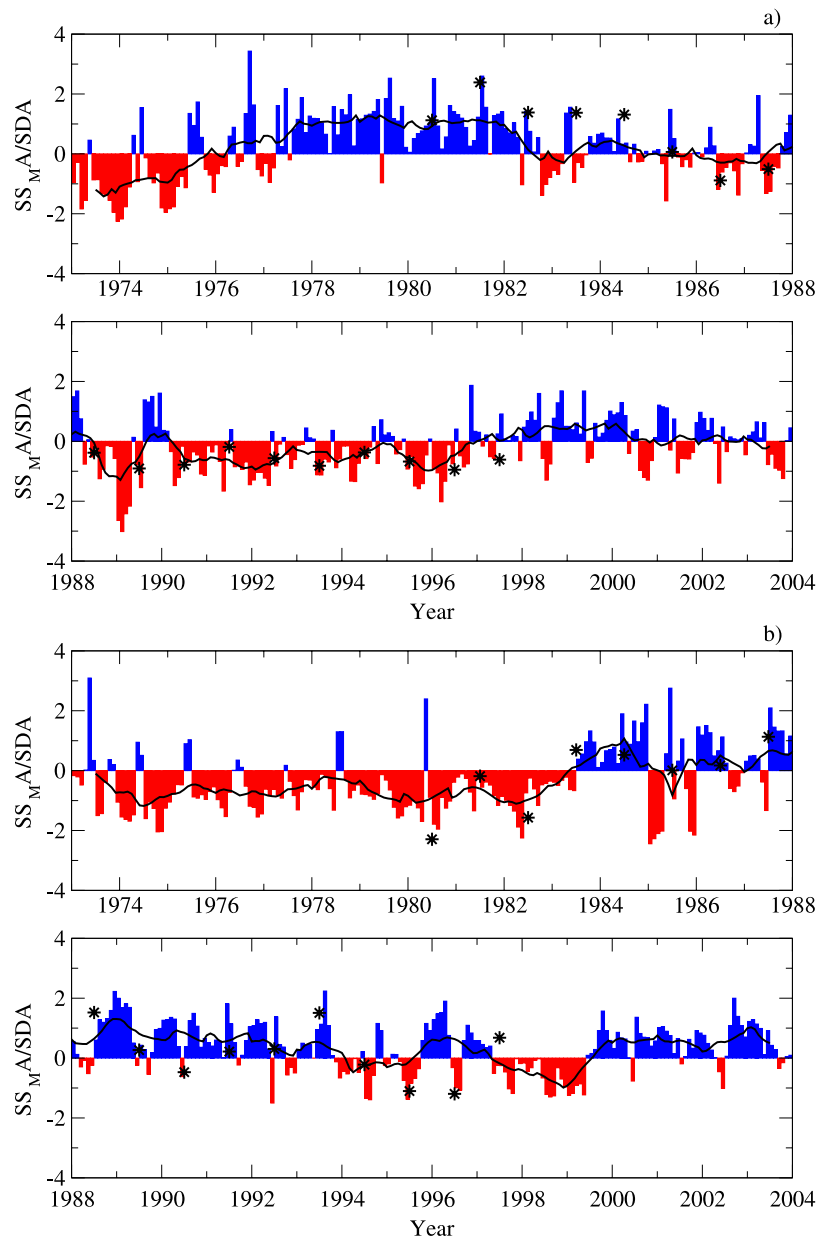


**Figure 3.** The 1980–1997 annual standardized maximum monthly SWE anomalies ( $SS_{M A}$ ; stars) and the 1973–2003 monthly standardized river discharge anomalies (SDA; bars) for (a) the Churchill River Basin and (b) the Chesterfield Inlet Basin. Blue (red) bars denote positive (negative) SDA values, and the black lines depict their 12-month running means.

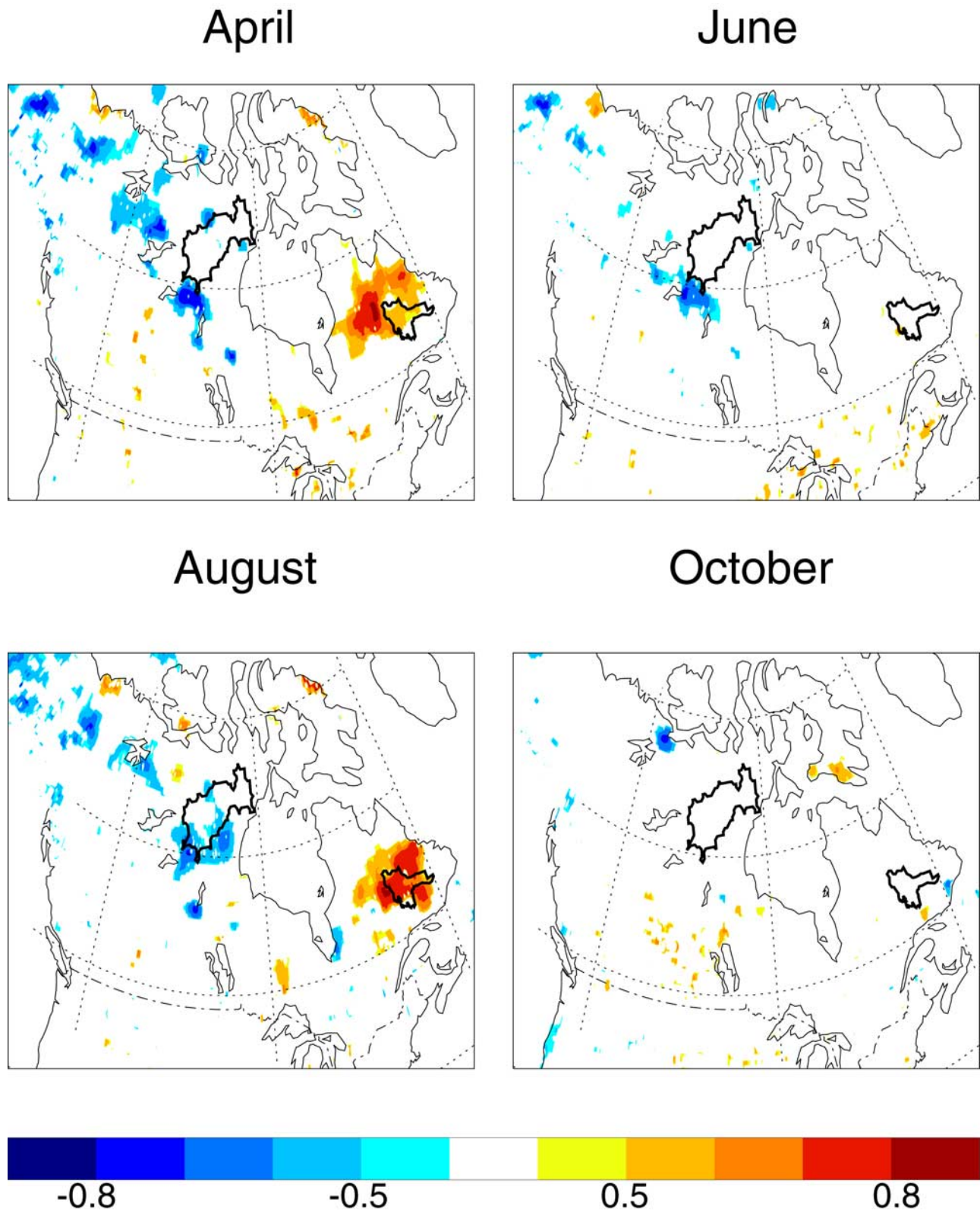


**Figure 4.** Correlation coefficient between the monthly standardized snow cover extent anomalies in Eurasia and the maximum SWE anomalies in Canada the following winter, 1980–1997. All correlations shown are statistically significant at the  $p < 0.05$  level. Thick black lines delineate the Churchill River and the Chesterfield Inlet Basins.

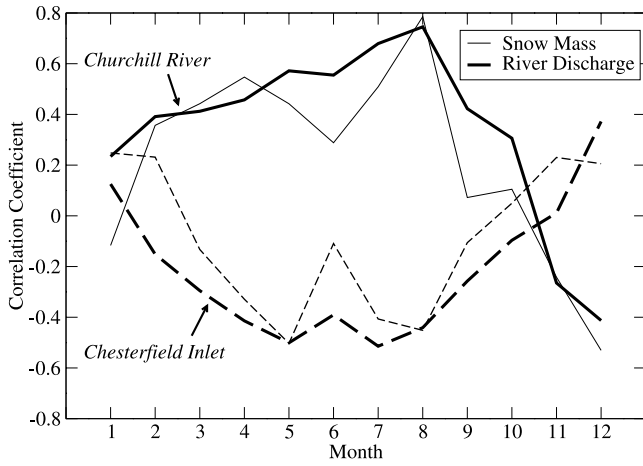


**Figure 5.** Correlation coefficient between the monthly standardized snow cover extent anomalies in Eurasia and the maximum SWE and river discharge anomalies the following year in the Churchill River and Chesterfield Inlet Basins, 1973–2003.

2003; Saunders et al., 2003; Gong et al., 2003a, 2003b]. There exist significant ( $p < 0.05$ ) positive (negative) correlations between spring and summer Eurasian snow cover extent anomalies and northeastern (northwestern) Canada maximum SWE anomalies the following winter. There is a decline in the strength of the correlations when computed with the June and October Eurasian snow cover extent anomalies. No significant correlations are observed in southern Canada and the United States. As an independent test, the calculations were repeated using the accumulated winter/spring (DJFMAM) precipitation from the Climate Research Unit of the University of East Anglia [New et al., 2000] instead of the SWE data. Strikingly similar patterns emerged in the correlation fields (not shown).

[23] Figure 5 depicts the correlation coefficient between monthly Eurasian snow cover extent anomalies and Churchill River and Chesterfield Inlet Basins annual maximum monthly SWE and annual river discharge anomalies the following year. In both basins, the correlation statistics for maximum SWE and river discharge match closely. This provides evidence of a coherent response to the forcing, with propagation from the snowpack to river discharge after snowmelt. For the Churchill River Basin, correlation values for maximum SWE ( $r = 0.79, p < 0.001$ ) and river discharge ( $r = 0.75, p < 0.001$ ) attain their peak values when computed with August Eurasian snow cover extent anomalies. In the Chesterfield Inlet Basin, the correlation values are not as significant, reaching values of  $r = -0.50$  ( $p = 0.03$ ) for SWE and  $r = -0.51$  ( $p = 0.004$ ) for river discharge when computed against May and July Eurasian snow cover extent anomalies, respectively. This plot also reveals the decrease in the significance of the correlations between the June Eurasian snow cover extent anomalies and the Canadian SWE anomalies seen in Figure 4. By October, the Eurasian snow cover extent anomalies are no longer significantly correlated to Canadian maximum SWE and river discharge anomalies and the correlations reverse signs by November but are not statistically significant. This may be an indication that Eurasian snow cover extent anomalies

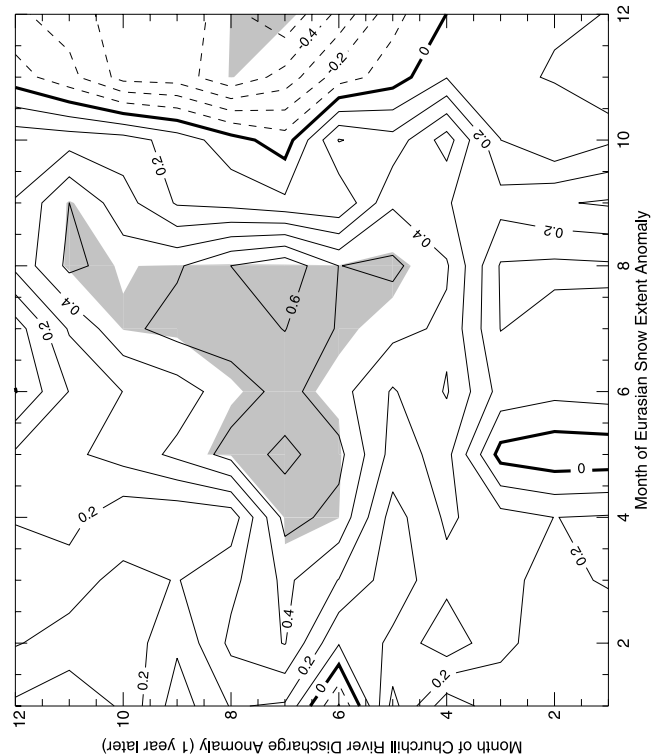
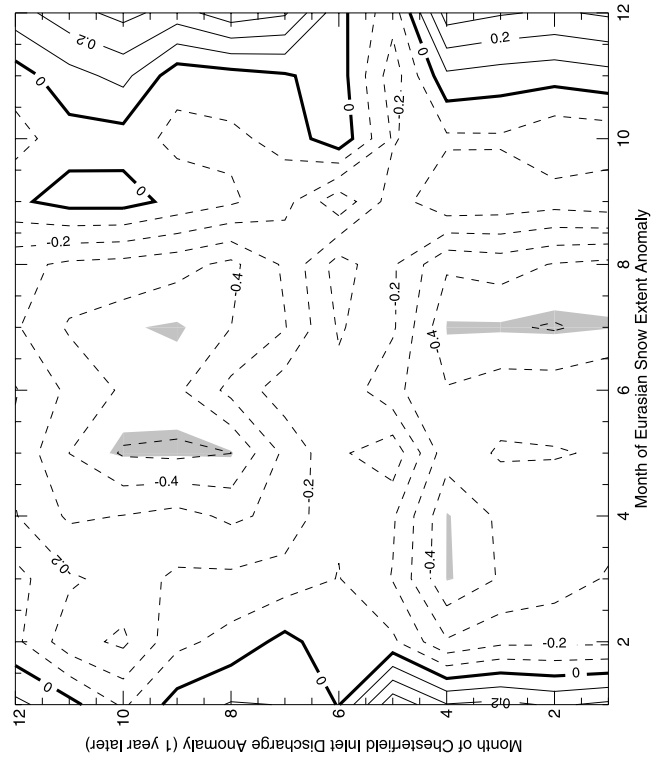


**Figure 6.** Correlation coefficient between the monthly standardized snow cover extent anomalies in Eurasia and the monthly freshwater discharge anomalies the following year in the Churchill River and Chesterfield Inlet Basins, 1973–2003. Gray shading denotes correlation coefficients that are statistically significant at the  $p < 0.01$  level.

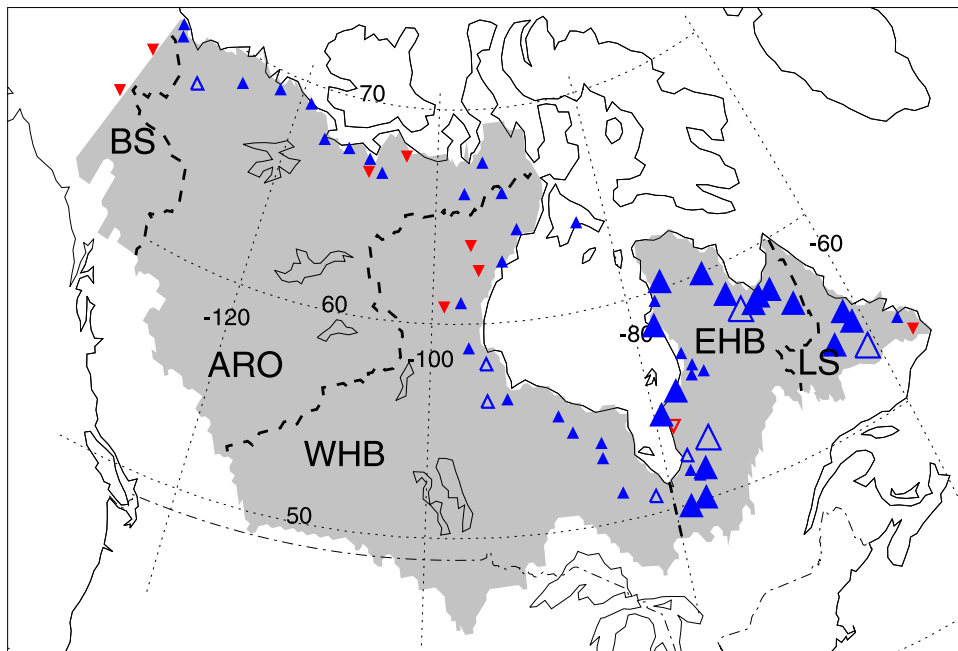


**Figure 7.** Correlation coefficient between the Eurasian annual standardized snow cover extent anomalies and the annual standardized discharge anomalies for 64 rivers of northern Canada (gray shading) the following year, 1973–2003. Positive (negative) correlations are denoted by blue (red) triangles, with statistically significant correlations ( $p < 0.05$ ) denoted by larger symbols. Open triangles denote rivers affected by major dams, diversions, and/or reservoirs. The symbols are located at the coordinates of the measuring gauge of each river nearest the outlet to high-latitude oceans. Dashed lines denote five regional basins of northern Canada (LS, Labrador Sea; EHB, Eastern Hudson Bay; WHB, Western Hudson Bay; ARO, Arctic Ocean; BS, Bering Strait).

have relatively less influence on Canadian SWE and river discharge anomalies owing to the diminished incoming solar radiation in the Northern Hemisphere during winter.

[24] Correlation coefficients between monthly Eurasian snow cover extent anomalies and monthly discharge anomalies in the Churchill River and Chesterfield Inlet Basins are shown in Figure 6. Eurasian snow cover extent anomalies from April to August correlate significantly ( $p < 0.01$ ) with monthly discharge rates in the Churchill River Basin from May to November the following year. Significant anticorrelations are less prominent for the Chesterfield Inlet Basin. Nonetheless, Eurasian snow cover extent anomalies from March to July do exhibit some significant anticorrelations with monthly Chesterfield Inlet freshwater discharge anomalies throughout the following year.

[25] The calculations are now generalized to 64 rivers of northern Canada for which hydrometric data are readily available [Déry and Wood, 2005]. Here, the correlations are based on the annual (rather than the monthly) Eurasian snow cover extent anomalies. Figure 7 demonstrates that river discharge into the Labrador Sea and Eastern Hudson Bay is strongly influenced by the preceding year Eurasian snow cover extent anomalies. Nineteen rivers of northern Quebec and Labrador, draining an area  $>0.6 \times 10^6 \text{ km}^2$  and with a mean annual total discharge of  $320 \text{ km}^3 \text{ yr}^{-1}$ , show statistically significant positive correlations. These rivers exhibit a spatially coherent response to the Eurasian snow cover extent anomalies. Significant anticorrelations are found in some of the rivers of Nunavut (including Chesterfield Inlet) when spring and/or summer Eurasian snow

cover extent anomalies are used in the calculations (not shown).

### 3.3. Pan-Arctic Response to Extreme Eurasian Snow Cover Extent Anomalies

[26] The connectivity in the pan-Arctic climate system is further investigated for 2 years with extreme Eurasian snow cover extent anomalies. Monthly Eurasian snow cover extent anomalies reach some of their largest and most persistent positive (negative) values in 1979 (1988) (see Figure 1). These 2 years are therefore chosen to contrast the atmospheric response to exceptional Eurasian snow cover extent anomalies and the effects on Canadian SWE and river discharge anomalies the following year.

[27] Figure 8 illustrates ERA-40 difference fields of winter/spring (DJFMAM) mean SLP, H5, SAT, and accumulated snowfall for 1979/80 minus 1988/89. Over most of the polar ice cap and northern Eurasia, positive SLP differences are observed, whereas two prominent negative SLP differences are found over the North Atlantic and North Pacific Oceans, typical of the negative phase of the AO. The polar region also experiences positive H5 differences, with centers of action near the North Pole and southern Greenland, whereas the adjacent annular band generally shows negative H5 differences. This H5 difference pattern marks another signature of the AO [Thompson and Wallace, 1998]. Positive snow cover extent anomalies in Eurasia lead to a local depression of SAT whereas positive SAT differences arise in northern Canada and Greenland. There is a marked response in Canadian precipitation (not shown) and snow-

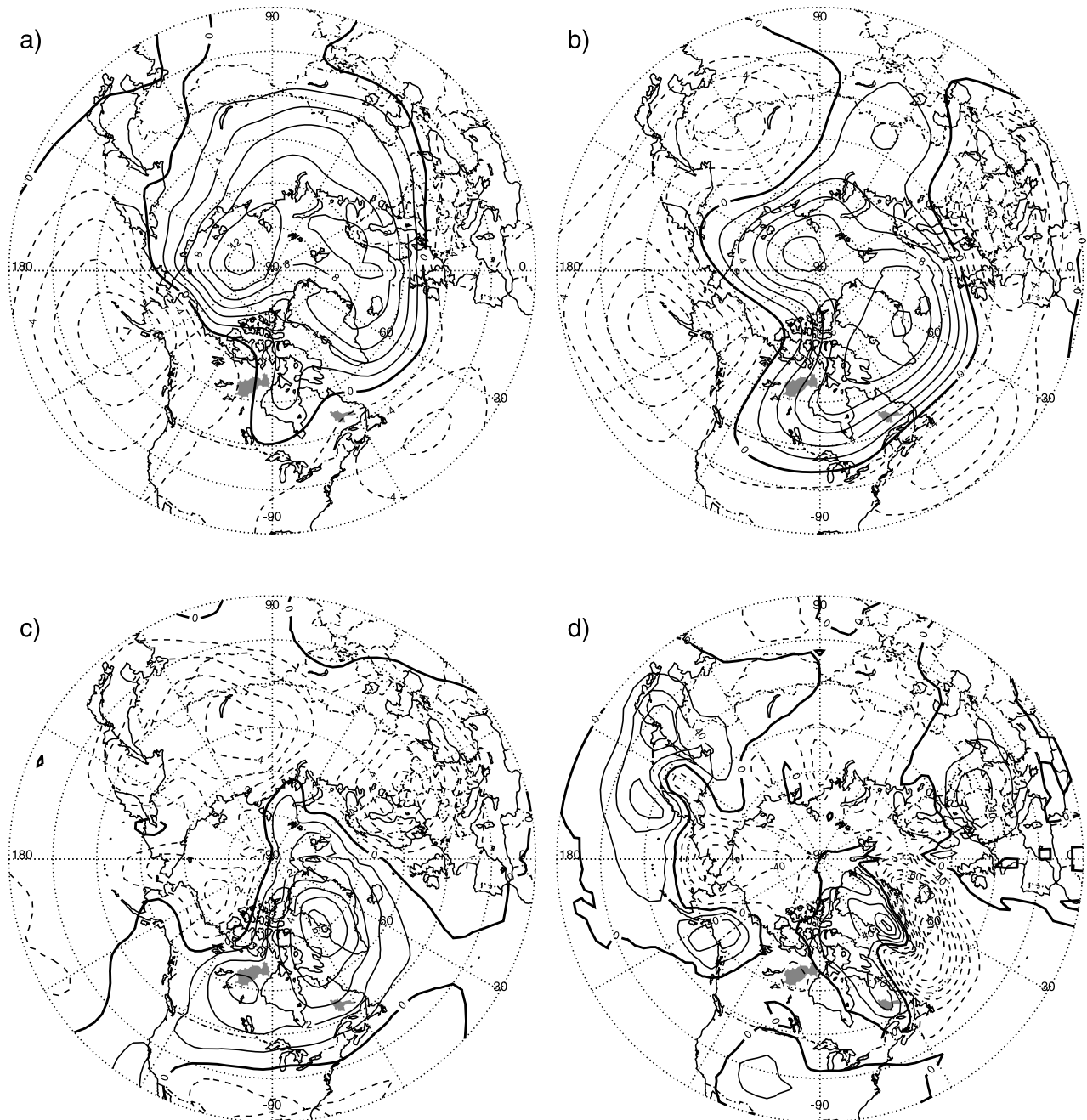


**Figure 8.** Difference (1979/80–1988/89) in ERA-40 Northern Hemisphere winter/spring (DJFMAM) (a) mean SLP (hPa), (b) mean H5 (dam), (c) mean SAT ( $^{\circ}\text{C}$ ), and (d) accumulated snowfall (mm SWE). The gray shading delineates the Churchill River and Chesterfield Inlet Basins.

fall to the Eurasian snow cover extent anomaly. Differences in snowfall are positive in eastern Canada and negative over central Canada. For the Churchill River and Chesterfield Inlet Basins, there is a difference of  $\approx 3^{\circ}\text{C}$  in SAT, but the response in terms of snowfall is of opposite sign. The Churchill River Basin receives  $\approx 40$  mm SWE of snowfall during the winter and spring of 1980 than 1989, whereas the Chesterfield Inlet Basin experiences a decline by  $\approx 20$  mm SWE. Although the change in SAT is about the same in the two watersheds, the hydrological response is quite different.

[28] Figure 9 depicts the difference (1980–1989) in the observed annual maximum monthly snow mass over

Canada. This shows the large positive (negative) SWE anomalies over northeastern (northwestern) Canada, consistent with the precipitation and snowfall anomalies during those years. Table 2 provides the areally averaged values of maximum SWE for both the Churchill River and Chesterfield Inlet Basins. There is a difference of 154 mm SWE in the maximum SWE observed in 1980 and that in 1989 for the Churchill River Basin and a modest decrease of 38 mm SWE in the Chesterfield Inlet Basin. These figures are consistent with the changes in freshwater discharge observed those 2 years (Table 2). Figure 10 presents differences (1980–1989) in the monthly standardized discharge

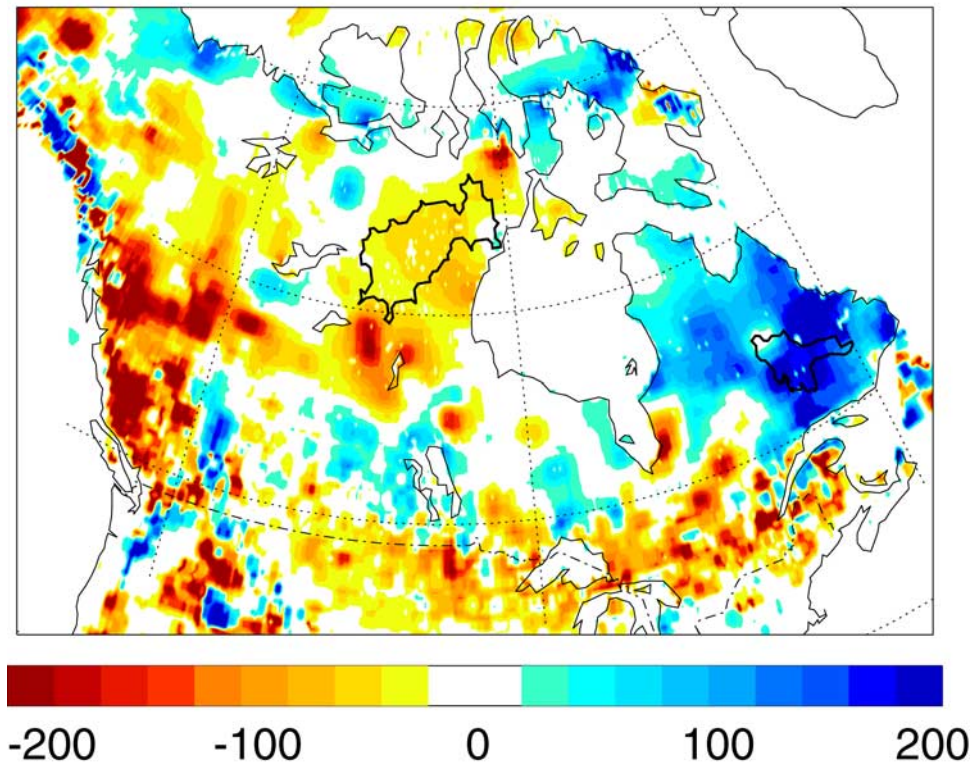


**Figure 9.** Difference (1980–1989) between the annual maximum monthly SWE (mm) in Canada. Thick black lines delineate the Churchill River and the Chesterfield Inlet Basins.

anomalies. Differences in the summer river discharge anomalies are consistent with the SWE anomalies observed during those years.

## 4. Discussion

### 4.1. Physical Mechanism of Pan-Arctic Climate Connectivity

[29] Several mechanisms have been proposed in the literature to explain the role of Eurasian snow cover extent anomalies on Northern Hemisphere atmospheric conditions. We review three mechanisms that emphasize the role of (1) Eurasian soil moisture, (2) North Atlantic sea surface temperatures (SSTs), and (3) polar wave flux activity, and then contend that (4) the persistent nature of Eurasian snow cover extent anomalies is critical to develop pan-Arctic climate connectivity.

#### 4.1.1. Eurasian Soil Moisture Anomalies

[30] Using the ECMWF model, *Barnett et al.* [1988, 1989] explored the impact of doubling or halving winter-time snowfall over Eurasia on global atmospheric conditions during spring. On the basis of their simulations, they argue that soil moisture anomalies associated with meltwa-

ter impose memory in the climate system to a greater degree than the snow albedo effect. Excessive snow mass acts as a heat sink through sublimation and melt processes and the subsequent soil moisture anomalies further exacerbate the thermal departures. As a consequence, SATs decrease and SLPs increase over Eurasia. A Rossby wave train ensues that manifests itself by positive SATs anomalies and negative SLP anomalies in North America during spring.

#### 4.1.2. North Atlantic SST Anomalies

[31] *Saunders et al.* [2003] suggest that positive summer snow cover extent anomalies in the zonal band 60°N to 70°N impose negative SAT anomalies over land and positive SAT anomalies over the subpolar North Atlantic. The resulting thermal winds yield positive SLP anomalies over the North Atlantic. Changes in midlatitude zonal winds then translate into positive SST anomalies over the North Atlantic that persist and weaken the AO/NAO the following winter.

#### 4.1.3. Polar Wave Flux Activity

[32] *Cohen and Entekhabi* [1999], *Saito et al.* [2001], and *Gong et al.* [2003a, 2003b] propose a different forcing mechanism altogether. They argue that positive snow cover extent anomalies during fall (SON) suppress overlying

**Table 2.** The 1980 and 1989 Annual River Discharge Rate  $D$  and the Annual Maximum Monthly SWE  $S_M$  for Two River Basins of Northern Canada

Basin	$D$ 1980, mm	$D$ 1989, mm	$\Delta D$ 1980–1989, mm	$S_M$ 1980, mm SWE	$S_M$ 1989, mm SWE	$\Delta S_M$ 1980–1989, mm SWE
Chesterfield Inlet	132.3	202.6	–70.3	54.6	92.9	–38.3
Churchill River	744.3	568.4	175.9	325.2	170.8	154.4

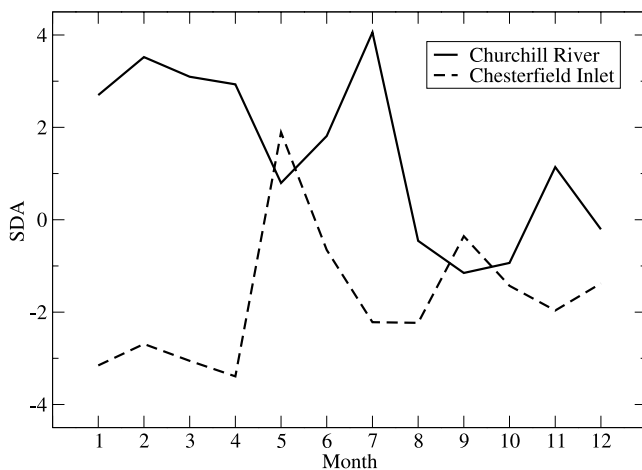


**Figure 10.** Difference (1980–1989) between the monthly standardized discharge anomalies (SDA) for the Churchill River and Chesterfield Inlet Basins.

SATs in Eurasia that enhance meridional temperature gradients. This amplified baroclinicity results in increased storminess and in large-scale Rossby wave activity over Eurasia. *Gong et al.* [2003a, 2003b] then suggest that an intensification of synoptic storms enhances vertical wave flux activity. This leads to the vertical transfer of energy toward the stratosphere that is subsequently refracted back toward the surface in the Northern Hemisphere polar region during winter. The AO then weakens and reverts to its negative phase owing to the enhanced downward motion near the North Pole.

#### 4.1.4. Persistence of Snow Cover Extent Anomalies

[33] Our study provides evidence that the previous three mechanisms may contribute to the observed pan-Arctic climate connectivity. First, the correlation statistics attained their most significant values when spring and summer Eurasian snow cover extent anomalies are used in the calculations (see Figure 4). This is in accord with the results of *Barnett et al.* [1988, 1989], *Saunders et al.* [2003], and *Bojariu and Gimeno* [2003]. However, the difference fields of SLP, H5, and SAT between the years (1979/80–1988/89) with positive and negative snow cover extent anomalies show a response similar to the model simulations analyzed by *Gong et al.* [2003a, 2003b].

[34] The Northern Hemisphere surface energy budget is most sensitive to snow cover extent anomalies during spring and early summer [*Groisman et al.*, 1994a, 1994b; *Pielke et al.*, 2000]. Strong solar insolation occurs at this time and relatively small spatial anomalies may lead to large fluctuations in the surface radiation budget owing to the snow cover's distinct characteristics. Thus the persistence of positive (negative) snow cover extent anomalies leads to an accumulated deficit (gain) in the surface radiation (water) budget of the Northern Hemisphere land surface that ultimately affects atmospheric conditions, including the AO/NAO, in subsequent years. Persistent snows may also induce lower than average summer SATs that herald the rapid advance of Eurasian snow cover extent during fall [e.g., *Leathers et al.*, 2002].

[35] The “run up and down test,” a nonparametric test to evaluate persistence in a time series [*Neter et al.*, 1993],

applied to the monthly Eurasian snow cover extent anomalies reveals that the hypothesis of randomness (as opposed to persistence) is rejected with confidence at the  $p < 0.001$  level. We can therefore state that Eurasian snow cover extent anomalies of a given sign tend to persist. This characteristic is further illustrated in Figure 11 that shows positive autocorrelation values of monthly Eurasian snow cover extent anomalies, particularly during spring and summer. In addition, Figure 1 shows a good example of a prolonged period with negative snow cover extent anomalies from 1988 to 1994. The “snow/albedo” feedback causes persistence of the snow cover extent anomalies that imposes a memory in the climate system lasting several months [*Cess et al.*, 1991; *Groisman et al.*, 1994a; *Walland and Simmonds*, 1997].

[36] We propose that persistent snow cover extent anomalies in Eurasia are the origin of the observed pan-Arctic climate connectivity. To test this hypothesis, we correlated values of the mean annual and seasonal Eurasian snow cover extent anomalies to the following winter (DJF) AO index values (Table 3). The AO is most significantly anticorrelated to mean annual Eurasian snow cover extent anomalies, with lesser correspondence to the seasonal values. Although this statistical analysis does not prove a causal relationship, it does suggest that persistent (rather than just transient) and expansive Eurasian snow cover extent anomalies may modulate the phase of the AO. Unlike *Saunders et al.* [2003] and *Cohen and Entekhabi* [1999] who find that summer and fall Eurasian snow cover extent anomalies, respectively, correlate more significantly to the NAO/AO, our results demonstrate that the mean annual values of Eurasian snow cover extent anomalies provide the most significant anticorrelations with the AO.

[37] For instance, large, positive snow cover extent anomalies in Eurasia persisted for 9 months from January to August of 1979, but then attained large, negative values in October and November. Despite the late fall negative snow cover extent anomalies, the AO retained its negative phase, in opposition to the anticipated response in the pan-Arctic climate system proposed by *Gong et al.* [2003a, 2003b]. Figure 12 depicts differences between 1976/77 and 1988/89 winter (DJF) SLP and SAT fields in the Northern Hemisphere. These two periods form the basis of the *Gong et al.* [2003a, 2003b] studies. Figure 12 shows a significant positive difference in SLP over the North Pole and the surrounding terrestrial regions. Large positive SAT differences are found over Canada and Greenland whereas large negative SAT differences occur in Eurasia. These spatial patterns are generally consistent with the modeling results of *Gong et al.* [2003a, 2003b]. However, the maximum positive difference in ERA-40 wintertime SLP of  $>28$  hPa is 23 hPa higher than the maximum value obtained in the ECHAM3 simulations. Similarly, the ERA-40 SAT differences are up to  $5^{\circ}\text{C}$  greater than represented by the ECHAM3 ensemble simulations.

[38] This provides evidence that large and persistent snow cover extent anomalies are required to develop the polar wave flux activity that impacts the AO as proposed by *Gong et al.* [2003a, 2003b]. A large positive Eurasian snow cover extent anomaly of short duration, such as in October 1976, may weaken the AO. The failure of the GCM simulations to reproduce the intensity of the atmospheric response to the

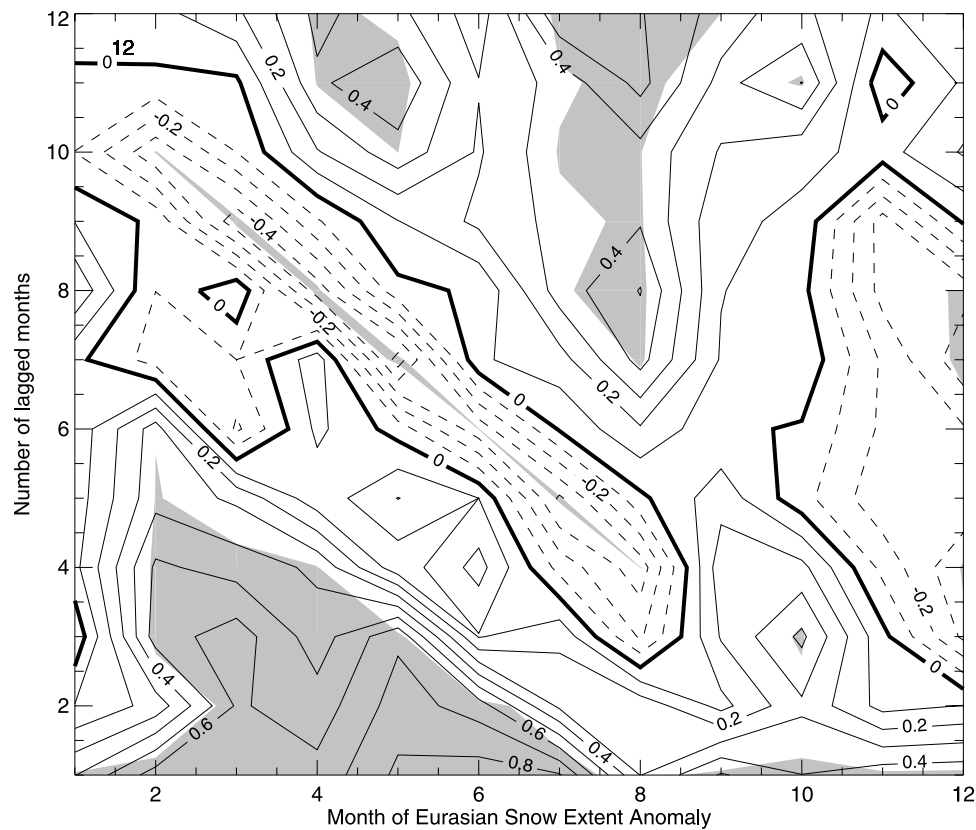


**Figure 11.** Autocorrelation of Eurasian monthly standardized snow cover extent anomalies for a given time lag (in months). Gray shading denotes correlation coefficients that are statistically significant at the  $p < 0.05$  level.

October 1976 Eurasian snow cover extent anomaly, however, suggests that longer time periods (including the antecedent spring and summer conditions) need to be considered to determine the degree of pan-Arctic climate connectivity.

#### 4.2. Predictability of Canadian SWE and River Discharge Anomalies

[39] This study provides compelling evidence of a statistical link between Eurasian snow cover extent anomalies and Canadian annual maximum monthly SWE and river discharge anomalies. Statistically significant correlations were found in both the Churchill River Basin of Labrador and the Chesterfield Inlet Basin of Nunavut, two large watersheds of northern Canada.

[40] The connectivity found in this study implies that Canadian SWE and freshwater discharge anomalies for a given year can be predicted on the basis of the state of Eurasian snow cover extent anomalies the preceding year. This has potential implications for water resources management in northern Canada. It is especially important for the Churchill River Basin and watersheds to the west (e.g., La Grande Rivière) where Newfoundland and Labrador Hydro and Hydro-Québec manage several large reservoirs that supply water for the generation of hydroelectricity [Déry and Wood, 2005]. For instance, a significant reduction in Eurasian snow cover extent during summer would alert power generation companies to manage their water resour-

ces conservatively in anticipation of a decline in wintertime precipitation, SWE, and river discharge the following year.

[41] Figure 4 also suggests that there exists several predictability “hot spots” in northern Canada. Apart from the Churchill River and Chesterfield Inlet Basins, significant anticorrelations between Eurasian snow cover extent anomalies and Canadian SWE are inferred in the northern regions of the Mackenzie River Basin, especially between Great Slave Lake and Great Bear Lake (perhaps owing to regional lake effects) as well as in central Alaska. Other hot spots of predictability may be masked given the relatively short time series (18 years) of observed SWE in Canada. The longer time series of river discharge reveal other areas where the terrestrial water budget may be predictable. Indeed, Figure 7 shows that the connectivity of the river

**Table 3.** Correlation Coefficient  $r$  Between the Mean Annual and Mean Seasonal Values of the Eurasian Standardized Snow Cover Extent Anomalies and the Following Winter (DJF) Arctic Oscillation Index, 1973–2000<sup>a</sup>

Period	$r$	$p$
Annual	-0.71	<0.001
Winter	-0.24	0.213
Spring	-0.45	0.017
Summer	-0.46	0.015
Fall	-0.59	<0.001

<sup>a</sup>Probability values  $p$  for the correlations are also listed.

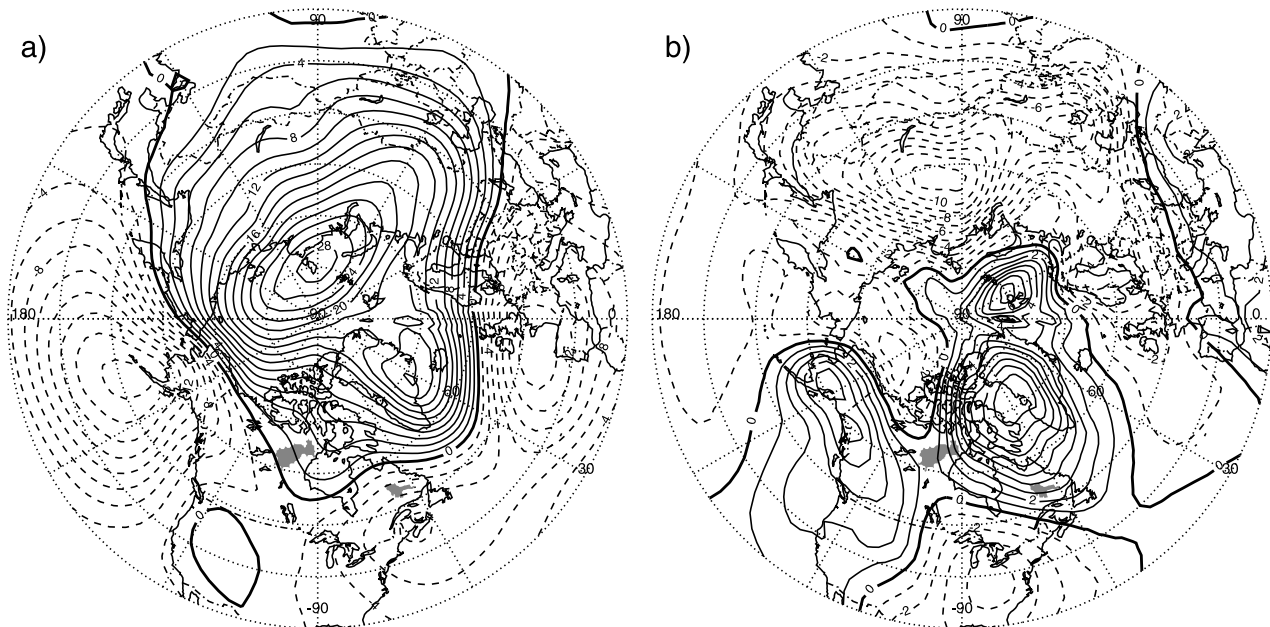


**Figure 12.** Difference (1976/77–1988/89) in ERA-40 Northern Hemisphere winter/spring (DJFMAM) (a) mean SLP (hPa) and (b) mean SAT ( $^{\circ}\text{C}$ ). The gray shading delineates the Churchill River and Chesterfield Inlet Basins.

discharge anomalies is spatially coherent with the SWE anomalies. There is a predominance of positive correlations in northeastern Canada and some anticorrelations in north central Canada. River discharge anomalies during spring and summer are therefore closely tied to the SWE anomalies and provide an indication as to the state of the wintertime precipitation and snow accumulation.

## 5. Summary

[42] This study reveals statistically significant positive (negative) correlations between spring and summer Eurasian standardized snow cover extent and maximum SWE and freshwater discharge in the Churchill River (Chesterfield Inlet) Basin of Canada. The correlation between August Eurasian standardized snow cover extent anomalies and Churchill River Basin maximum SWE and river discharge anomalies the following year attained  $r = 0.79$  and  $r = 0.75$ , respectively. Anticorrelations in the Chesterfield Inlet Basin were less significant, with values of  $r = -0.50$  and  $r = -0.51$  for maximum SWE and river discharge anomalies, respectively. Nineteen rivers draining more than  $0.6 \times 10^6 \text{ km}^2$  of northern Quebec and Labrador and with a mean annual total discharge of  $320 \text{ km}^3 \text{ yr}^{-1}$  show statistically significant positive correlations to the annual Eurasian standardized snow cover extent anomalies. This pan-Arctic climate connectivity is related to the persistent nature of the Eurasian snow cover extent anomalies and the associated accumulated gains or deficits in the surface radiation and water budgets that impose a memory in the climate system, including the AO. The state of the surface water budget in the Churchill River and Chesterfield Inlet Basins may therefore be predictable up to 1 year in advance owing to the observed pan-Arctic climate connectivity.

[43] A suite of GCM simulations of 21st century climate under different scenarios suggests that Eurasian snow will

retreat in spatial extent [e.g., *Ye and Mather, 1997; Holland and Bitz, 2003; Frei and Gong, 2005*]. Extrapolating our results, this implies that northeastern (northwestern) Canada will continue to experience below (above) average SWE and river discharge. An analysis of the GCM simulations that are participating in the IPCC fourth assessment will be conducted to determine whether climate models are able to reproduce the observed pan-Arctic climate connectivity and how climate change may impact the pan-Arctic terrestrial water budget.

[44] **Acknowledgments.** We thank M. Stieglitz (Georgia Tech) and E. McKenna for their contributions to this work, R. Brown, (Environment Canada) who generously provided the snow water equivalent data, and D. P. Lettenmaier and three anonymous referees for their useful comments. This project has been funded through support from grant NSF OPP02-30211 (Collaborative research: The role of spatial and temporal variability of pan-Arctic river discharge and surface hydrological processes on climate) to E. F. Wood. This report was prepared by S. J. Déry under award NA17RJ2612 from National Oceanic and Atmospheric Administration (NOAA), U.S. Department of Commerce. The statements, findings, conclusions, and recommendations are those of the authors and do not necessarily reflect the views of NOAA or the U.S. Department of Commerce.

## References

- Bamzai, A. S. (2003), Relationship between snow cover variability and Arctic Oscillation on a hierarchy of time scales, *Int. J. Climatol.*, **23**, 131–142, doi:10.1002/joc.854.
- Bamzai, A. S., and J. Shukla (1999), Relation between Eurasian snow cover, snow depth, and the Indian summer monsoon: An observational study, *J. Clim.*, **12**, 3117–3132.
- Barnett, T. P., L. Dümenil, U. Schlese, and E. Roeckner (1988), The effect of Eurasian snow cover on global climate, *Science*, **239**, 504–507.
- Barnett, T. P., L. Dümenil, U. Schlese, E. Roeckner, and M. Latif (1989), The effect of Eurasian snow cover on regional and global climate variations, *J. Atmos. Sci.*, **46**, 661–685.
- Bojariu, R., and L. Gimeno (2003), The role of snow cover fluctuations in multiannual NAO persistence, *Geophys. Res. Lett.*, **30**(4), 1156, doi:10.1029/2002GL015651.
- Brown, R. D., B. Brasnett, and D. Robinson (2003), Gridded North American monthly snow depth and snow water equivalent for GCM evaluation, *Atmos. Ocean*, **41**, 1–14.

- Cess, R. D., et al. (1991), Interpretation of snow-climate feedback as produced by 17 general circulation models, *Science*, *253*, 888–892.
- Cohen, J., and D. Entekhabi (1999), Eurasian snow cover variability and Northern Hemisphere climate predictability, *Geophys. Res. Lett.*, *26*, 345–348.
- Cohen, J., and D. Rind (1991), The effect of snow cover on the climate, *J. Clim.*, *4*, 689–706.
- Cohen, J. L., and K. Saito (2003), Eurasian snow cover, more skillful in predicting U.S. winter climate than the NAO/AO?, *Geophys. Res. Lett.*, *30*(23), 2190, doi:10.1029/2003GL018053.
- Derksen, C., A. Walker, and B. Goodison (2005), Evaluation of passive microwave snow water equivalent retrievals across the boreal forest/tundra transition of western Canada, *Remote Sens. Environ.*, *96*, 315–327.
- Déry, S. J., and E. F. Wood (2004), Teleconnection between the Arctic Oscillation and Hudson Bay river discharge, *Geophys. Res. Lett.*, *31*, L18205, doi:10.1029/2004GL020729.
- Déry, S. J., and E. F. Wood (2005), Decreasing river discharge in northern Canada, *Geophys. Res. Lett.*, *32*, L10401, doi:10.1029/2005GL022845.
- Déry, S. J., and M. K. Yau (2002), Large-scale mass balance effects of blowing snow and surface sublimation, *J. Geophys. Res.*, *107*(D23), 4679, doi:10.1029/2001JD001251.
- Déry, S. J., W. T. Crow, M. Stieglitz, and E. F. Wood (2004), Modeling snow-cover heterogeneity over complex Arctic terrain for regional and global climate models, *J. Hydrometeorol.*, *5*, 33–48.
- Déry, S. J., V. V. Salomonson, M. Stieglitz, D. K. Hall, and I. Appel (2005a), An approach to using snow areal depletion curves inferred from MODIS and its application to land surface modelling in Alaska, *Hydrol. Proc.*, *19*, 2755–2774, doi:10.1002/hyp.5784.
- Déry, S. J., M. Stieglitz, A. K. Rennermalm, and E. F. Wood (2005b), The water budget of the Kuparuk River Basin, Alaska, *J. Hydrometeorol.*, *6*, 633–655.
- Déry, S. J., M. Stieglitz, E. C. McKenna, and E. F. Wood (2005c), Characteristics and trends of river discharge into Hudson, James, and Ungava Bays, 1964–2000, *J. Clim.*, *18*, 2540–2557.
- Dye, D. G. (2002), Variability and trends in the annual snow-cover cycle in Northern Hemisphere land area, 1972–2000, *Hydrol. Processes*, *16*, 3065–3077.
- Ellis, A. W., and D. J. Leathers (1998), The effects of a discontinuous snow cover on lower atmospheric temperature and energy flux patterns, *Geophys. Res. Lett.*, *25*, 2161–2164.
- Frei, A., and G. Gong (2005), Decadal to century scale trends in North American snow extent in coupled atmosphere-ocean general circulation models, *Geophys. Res. Lett.*, *32*, L18502, doi:10.1029/2005GL023394.
- Frei, A., and D. A. Robinson (1999), Northern Hemisphere snow extent: Regional variability 1972–1994, *Int. J. Climatol.*, *19*, 1535–1560.
- Gong, G., D. Entekhabi, and J. Cohen (2003a), Relative impacts of Siberian and North American snow anomalies on the winter Arctic Oscillation, *Geophys. Res. Lett.*, *30*(16), 1848, doi:10.1029/2003GL017749.
- Gong, G., D. Entekhabi, and J. Cohen (2003b), Modeled Northern Hemisphere winter climate response to realistic Siberian snow anomalies, *J. Clim.*, *16*, 3917–3931.
- Groisman, P. Y., T. R. Karl, and R. W. Knight (1994a), Observed impact of snow cover on the heat balance and the rise of continental spring temperatures, *Science*, *263*, 198–200.
- Groisman, P. Y., T. R. Karl, R. W. Knight, and G. L. Stenchikov (1994b), Changes of snow cover, temperature, and radiative heat balance over the Northern Hemisphere, *J. Clim.*, *7*, 1633–1656.
- Hahn, D. G., and J. Shukla (1976), An apparent relationship between Eurasian snow cover and Indian summer monsoon rainfall, *J. Atmos. Sci.*, *33*, 2461–2462.
- Holland, M. M., and C. M. Bitz (2003), Polar amplification of climate change in coupled models, *Clim. Dyn.*, *21*, 221–232, doi:10.1007/s00382-003-0332-6.
- Hurrell, J. W. (1995), Decadal trends in the North Atlantic Oscillation: Regional temperatures and precipitation, *Science*, *269*, 676–679.
- Leathers, D. J., et al. (2002), Associations between continental-scale snow cover anomalies and air mass frequencies across eastern North America, *Int. J. Climatol.*, *22*, 1473–1494.
- McNamara, J. P., D. L. Kane, and L. D. Hinzman (1998), An analysis of streamflow hydrology in the Kuparuk River Basin, Alaska: A nested watershed approach, *J. Hydrol.*, *206*, 39–57.
- Neter, J., W. Wasserman, and G. A. Whitmore (1993), *Applied Statistics*, 4th ed., 989 pp., Allyn and Bacon, Needham Heights, Mass.
- New, M., M. Hulme, and P. Jones (2000), Representing twentieth-century space-time climate variability. part II: Development of 1901–96 monthly grids of terrestrial surface climate, *J. Clim.*, *13*, 2217–2238.
- Peterson, B. J., et al. (2002), Increasing river discharge to the Arctic Ocean, *Science*, *298*, 2171–2173.
- Pielke, R. A., Sr., G. E. Liston, and A. Robock (2000), Insolation-weighted assessment of Northern Hemisphere snow-cover and sea-ice variability, *Geophys. Res. Lett.*, *27*, 3061–3064.
- Qian, B. D., and M. A. Saunders (2003), Seasonal predictability of wintertime storminess over the North Atlantic, *Geophys. Res. Lett.*, *30*(13), 1698, doi:10.1029/2003GL017401.
- Robinson, D. A., and A. Frei (2000), Seasonal variability of Northern Hemisphere snow extent using visible satellite data, *Prof. Geogr.*, *52*, 307–315.
- Saito, K., and J. Cohen (2003), The potential role of snow cover in forcing interannual variability of the major Northern Hemisphere mode, *Geophys. Res. Lett.*, *30*(6), 1302, doi:10.1029/2002GL016341.
- Saito, K., J. Cohen, and D. Entekhabi (2001), Evolution of atmospheric response to early-season Eurasian snow cover anomalies, *Mon. Weather Rev.*, *129*, 2746–2760.
- Saunders, M. A., B. D. Qian, and B. Lloyd-Hughes (2003), Summer snow extent heralding of the winter North Atlantic Oscillation, *Geophys. Res. Lett.*, *30*(7), 1378, doi:10.1029/2002GL016832.
- Schaefer, A., A. S. Denning, and O. Leonard (2004), The winter Arctic Oscillation and the timing of snowmelt in Europe, *Geophys. Res. Lett.*, *31*, L22205, doi:10.1029/2004GL021035.
- Shinoda, M. (2001), Climate memory of snow mass as soil moisture over central Eurasia, *J. Geophys. Res.*, *106*, 33,393–33,403.
- Stieglitz, M., A. Ducharme, R. Koster, and M. Suarez (2001), The impact of detailed snow physics on the simulation of snow cover and subsurface thermodynamics at continental scales, *J. Hydrometeorol.*, *2*, 228–242.
- Stieglitz, M., S. J. Déry, V. E. Romanovsky, and T. E. Osterkamp (2003), The role of snow cover in the warming of Arctic permafrost, *Geophys. Res. Lett.*, *30*(13), 1721, doi:10.1029/2003GL017337.
- Thompson, D. W. J., and J. M. Wallace (1998), The Arctic Oscillation signature in the wintertime geopotential height and temperature fields, *Geophys. Res. Lett.*, *25*, 1297–1300.
- Walland, D. J., and I. Simmonds (1997), North American and Eurasian snow cover co-variability, *Tellus, Ser. A*, *49*, 503–512.
- Wang, L., M. Sharp, R. Brown, C. Derksen, and B. Rivard (2005), Evaluation of spring snow covered area depletion in the Canadian Arctic from NOAA snow charts, *Remote Sens. Environ.*, *95*, 453–463.
- Watanabe, M., and T. Nitta (1998), Relative impacts of snow and sea surface temperature anomalies on an extreme phase in the winter atmospheric circulation, *J. Clim.*, *11*, 2837–2857.
- Watanabe, M., and T. Nitta (1999), Decadal changes in the atmospheric circulation and associated surface climate variations in the Northern Hemisphere winter, *J. Clim.*, *12*, 494–510.
- Ye, H., and J. R. Mather (1997), Polar snow cover changes and global warming, *Int. J. Climatol.*, *17*, 155–162.
- Yeh, T. C., R. T. Wetherald, and S. Manabe (1983), A model study of the short term climatic and hydrologic effects of sudden snow-cover removal, *Mon. Weather Rev.*, *111*, 1013–1024.
- Zishka, K. M., and P. J. Smith (1980), The climatology of cyclones and anticyclones over North America and surrounding ocean environs for January and July, 1955–77, *Mon. Weather Rev.*, *108*, 387–401.

S. J. Déry, Environmental Science and Engineering Program, University of Northern British Columbia, 3333 University Way, Prince George, BC, Canada V2N 4Z9. (sdery@unbc.ca)

J. Sheffield and E. F. Wood, Department of Civil and Environmental Engineering, Princeton University, Princeton, NJ 08544, USA.